

*TRANSIENTS IN THREE-LEVEL MASERS*

A. A. MANENKOV, R. M. MARTIROSYAN, Yu. P. PIMENOV, A. M. PROKHOROV, and V. A. SYCHUGOV

P. N. Lebedev Physics Institute, Academy of Sciences, U.S.S.R.

Submitted to JETP editor May 14, 1964

J. Exptl. Theoret. Phys. (U.S.S.R.) **47**, 2055-2063 (December, 1964)

An experimental and theoretical investigation is made of the process of establishment of the amplitude of oscillation in three-level paramagnetic masers. The experiments were carried out on masers utilizing ruby and rutile crystals containing  $\text{Cr}^{3+}$ . The maser radiation was at 21 and 10 cm, respectively. With pulsed pumping a transient is observed consisting of amplitude-damped oscillations and subsequent exponential approach to steady-state conditions. The theoretical analysis of the transients is carried out on the basis of the rate equations for the three-level model. A solution of these equations in the linear approximation is obtained in analytical form. Formulas are also derived for the time elapsing between the beginning of pumping and the start of oscillations. The theoretical calculations are in good agreement with the experimental data.

**1. INTRODUCTION**

RECENTLY several papers have been published<sup>[1-14]</sup> dealing with the theoretical and experimental investigation of transients in masers. The majority of these are concerned with optical masers (lasers) and two-level radio-frequency masers. Only one paper<sup>[4]</sup> was devoted to an investigation of transients in a three-level rf maser (ruby); however, even in this case the theoretical analysis was carried out on the basis of a two-level scheme, which strictly speaking is inadequate for the description of three-level oscillators.

The purpose of the present work was a detailed experimental investigation and theoretical analysis of transients in three-level rf masers—paramagnetic masers (PM). Such an investigation is also of interest for lasers. The process of establishment of oscillations in crystal lasers can have much in common with the transients in PM. In both cases population inversion is produced by external auxiliary radiation (the pump). When pulsed pumping is used, transients can be observed with appreciable oscillations of amplitude. In lasers working in the pulsed mode the emission usually has a spiky character with regular or irregular spikes. The theoretical analysis of such processes in lasers is very complicated because the laser resonator is essentially a multi-mode system in which several modes of oscillations can be excited, either with a time delay or simultaneously. The spiky mode of lasers can be associated with the excitation of several types of oscillations and

can probably be represented as a complex superposition of transients for separate modes.<sup>[12]</sup> In certain specific cases, a spikeless mode is observed in lasers, with simple decaying transient oscillations and a constant-amplitude output in the steady state,<sup>[11]</sup> which has a rather simple theoretical interpretation.

In the case of masers we have to do with a single-mode resonator (at the generated frequency), which greatly simplifies the theoretical analysis and permits a more detailed study to be made of the transients than in lasers. In addition, in the case of PM the investigation of these processes is facilitated because it is easy to form perfect rectangular pump pulses at radio frequencies.

**2. EXPERIMENTAL RESULTS**

We investigated the transient processes in two PM's using crystals of ruby and rutile ( $\text{TiO}_2$ ) doped with  $\text{Cr}^{3+}$ . These masers were in the form of self-excited, single-cavity (at the signal frequency) paramagnetic amplifiers, similar to those described earlier.<sup>[15,16]</sup> The ruby radiated at about 21 cm, the rutile at about 10 cm. The wavelengths of the pumps were about 2.7 cm and 0.8 cm respectively. The energy levels of the  $\text{Cr}^{3+}$  ion in the crystals of  $\text{Al}_2\text{O}_3$  and  $\text{TiO}_2$  utilized in the masers are shown in Fig. 1. The  $\text{Cr}^{3+}$  ion concentration in the crystals was 0.03% in the  $\text{Al}_2\text{O}_3$  and 0.06% in the  $\text{TiO}_2$ . In both masers the external magnetic field (intensity about 2000 G) was provided by superconducting magnets, resulting in extremely

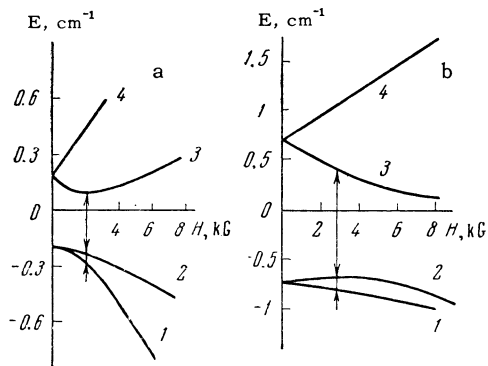


FIG. 1.  $\text{Cr}^{3+}$  energy levels: a – in  $\text{Al}_2\text{O}_3$  (magnetic field  $H$  perpendicular to the crystal  $C$  axis); b – in  $\text{TiO}_2$  (magnetic field  $H$  parallel to the crystal  $C$  axis). The arrows show the pump (1  $\rightarrow$  3) and signal (2  $\rightarrow$  1) transitions used in the masers.

stable operation of the masers. Both masers were operated at  $4.2^\circ\text{K}$ . Semiconducting diodes in the high-frequency circuit were used to modulate the pump power. The pump pulses were rectangular in shape with a rise time for the leading and trailing fronts  $< 3 \mu\text{sec}$ . The pulse lengths were varied in the interval from several microseconds to several tens of milliseconds. Variation of the pump power  $P$  permitted investigation of the transients for values of  $P/P_0$  from 1 to 16, where  $P_0$  is the threshold power. Several typical oscillograms of transients observed in the ruby and rutile PM's are shown in Figs. 2 and 3.

Figure 2a shows the complete transient oscillation amplitude in the ruby PM during a pump pulse of length  $\tau_p = 45 \text{ msec}$ , with a pump power several times greater than the threshold value.

Figure 2b shows the time scan of the beginning of the transient for  $\tau_p = 3.5 \text{ msec}$ . In Fig. 2c is shown the oscillation regime with the pump power near threshold and  $\tau_p = 50 \text{ msec}$ . It can be seen in this oscillogram that oscillations (first peak) begin later than the beginning of the pump pulse, which coincides with the beginning of the oscilloscope trace. The lag in this case is 18 msec.

In Figs. 3a, b, and c, which pertain to the rutile maser, the rectangular pulses of the pump are shown simultaneously with the signal in order to make time comparisons. The oscillograms in Figs. 3a and b were obtained with the same power, but with different pump pulse lengths (570 and 200  $\mu\text{sec}$ , respectively). In Fig. 3c  $\tau_p = 100 \mu\text{sec}$ , and the pump power is less than in Figs. 3a and b. In this figure it is seen that the oscillations lag the beginning of the pump pulse by a time  $t_3 = 50 \mu\text{sec}$ . In Fig. 3d the start of the transient in the rutile maser is shown on an expanded time scale.

Thus it can be seen from these oscillograms that in the ruby and rutile masers the establishment of oscillation amplitude has the character of damped transient oscillations with subsequent exponential approach to the steady-state condition with constant amplitude (for a sufficiently large excess over the threshold). Attention is directed to the fact that the various stages of the transient process are substantially different in the ruby and rutile masers. These differences are the following:

1. The amplitude of the transient oscillations  $A$  (as compared with the steady-state amplitude  $A_0$ ) is much greater in the ruby maser. For the ruby

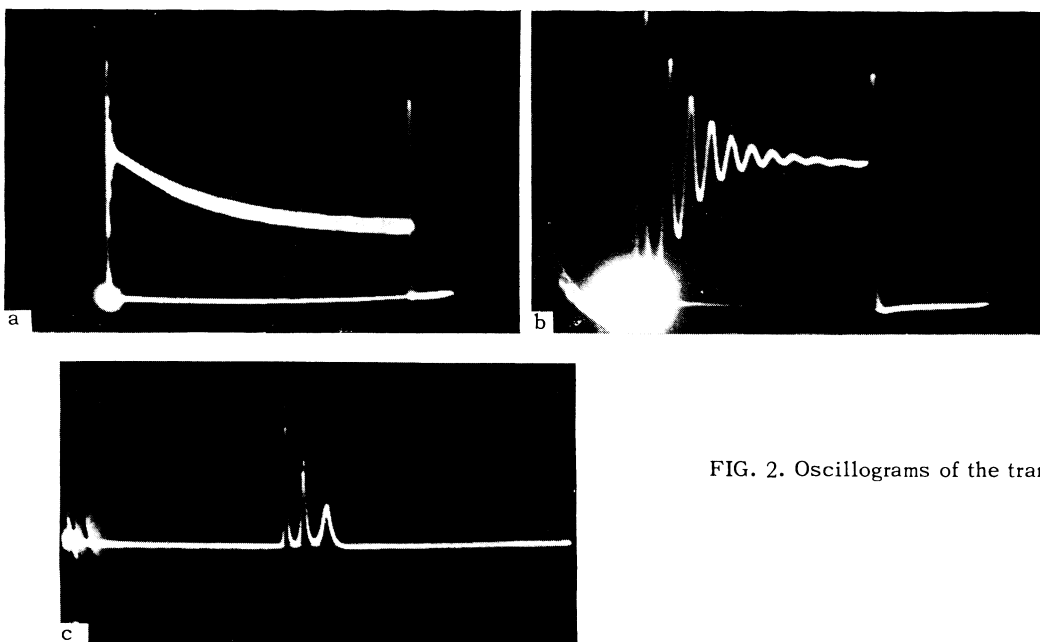


FIG. 2. Oscillograms of the transient in the ruby maser.

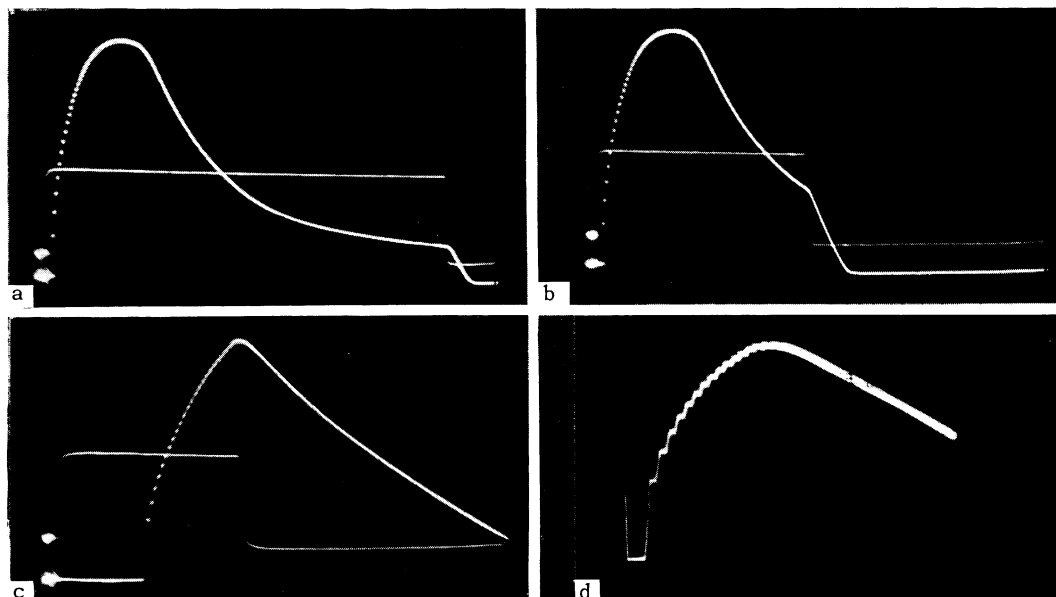


FIG. 3. Oscillograms of the transient in the rutile maser.

maser  $A_{\max} > A_0$ , whereas in the rutile maser  $A_{\max} < A_0$  for all the values of pump power used in the experiments.

2. All times that characterize the separate stages of the transient—the delay time  $t_d$  by which the initiation of oscillation lags the beginning of the pump pulse, the period  $T_{\text{osc}}$  and the decay time  $\tau$  of the oscillations, the time  $\tau_e$  of the exponential approach to the steady state (after the oscillations have decayed)—are much shorter in the rutile maser. Thus, for the same excess of pump power over the threshold  $P/P_0 = 3$  for both masers, we have for the rutile maser  $t_d \approx 280 \mu\text{sec}$ , whereas for the ruby maser  $t_d = 4 \text{ msec}$ . For  $T_{\text{osc}}$  and  $\tau_e$ , measured for  $P/P_0 = 10$ , we have:  $T_{\text{osc}} \approx 2 \mu\text{sec}$ ,  $\tau_e \approx 100 \mu\text{sec}$  in the rutile maser,  $T_{\text{osc}} \approx 70 \mu\text{sec}$ ,  $\tau_e = 10 \text{ msec}$  in the ruby maser. The quantities  $t_d$ ,  $T_{\text{osc}}$ ,  $\tau$ , and  $\tau_e$  depend on the pump power. The experimental data obtained in the investigation of this dependence are presented below in the comparison with theory.

3. At the moment the pump pulse is turned off in the ruby maser there is observed a sharp oscillation spike, the length of which is approximately the same as the length of the first peak in the initial transient oscillations (see Fig. 2b). The amplitude of this end peak decreases when the pump power is reduced, and for a small excess over the threshold, it disappears completely. In the rutile laser the character of the damping of the oscillations after the pump pulse is turned off is different: a smooth fall-off in the oscillation amplitude is observed (see Figs. 3a, b, c).

4. The output powers of the ruby and rutile masers are very different—in steady state the maximum power of the ruby maser was about  $10^{-7} \text{ W}$ , whereas for the rutile maser it was about  $10^{-5} \text{ W}$ .

### 3. THEORY. COMPARISON WITH EXPERIMENT

The theoretical analysis of the observed transient processes in PM's can be carried out on the basis of rate equations similar to the equations of Statz and de Mars,<sup>[4]</sup> after generalizing them to the three-level case. The basis of applicability of the rate equation method to the analysis of transients in crystal masers has been given by Tang,<sup>[13]</sup> who showed that in the case when  $T_2^{-1} \gg T_1^{-1}$ ,  $\gamma_0$ , where  $T_2$  is the spin-spin relaxation time,  $T_1$  is the spin-lattice relaxation time, and  $\gamma_0$  is the width of the resonator line, the exact equations for the density matrix and the electromagnetic field can be reduced to the rate equations of Statz and de Mars. These conditions are satisfied for both masers and lasers.

We consider a system of paramagnetic ions having three energy levels  $E_3 > E_2 > E_1$ . We assume that the pump radiation at frequency  $\nu_{31} = (E_3 - E_1)/h$  creates an inversion of the populations of levels 2 and 1 so that emission can arise in the transition  $2 \rightarrow 1$ . Then the three-level maser can be described by the system of rate equations

$$\begin{aligned} \dot{x} = & -(a_2 + 2a_3)(x - x_p) \\ & + (a_1 - a_2)(\delta - \delta_p) + W\delta - 2xy, \end{aligned}$$

$$\begin{aligned} \dot{\delta} &= (a_3 - a_2)(x - x_p) - (2a_1 + a_2)(\delta - \delta_p) - 2W\delta + xy, \\ \dot{y} &= \alpha xy - y/\tau_p, \end{aligned} \quad (1)$$

where  $x = n_2 - n_1$  and  $\delta = n_1 - n_3$  are the population differences for the signal ( $2 \rightarrow 1$ ) and pump ( $1 \rightarrow 3$ ) transitions respectively,  $x_p$  and  $\delta_p$  are these population differences at Boltzmann equilibrium (for  $W = 0$ ,  $y = 0$ );  $W$  and  $y$  are the transition probabilities of the  $1 \rightarrow 3$  and  $2 \rightarrow 1$  transitions induced respectively by the field of the external auxiliary radiation (the pump) and the field of the maser radiation itself;  $a_1$ ,  $a_2$ ,  $a_3$  are the probabilities of relaxation transitions between levels  $1 \rightarrow 3$ ,  $2 \rightarrow 3$ , and  $2 \rightarrow 1$ , respectively;  $\alpha$  is a parameter specifying the effectiveness of the interaction of the spin system with the radiation field of the maser at frequency  $\nu_{21}$ ;  $\tau_p = Q/\omega$  is the characteristic time of a resonator having quality factor  $Q$  at the frequency  $\nu_{21} = \omega/2\pi$ . The power radiated by the active substance is

$$P_{\text{rad}} = h\nu_{21}xy. \quad (2)$$

The solution of the system of nonlinear equations (1) can be obtained by numerical methods (e.g., on a computer); however, several important results can be obtained by solving them in a linear approximation. The solution of the linearized system can be obtained in analytical form, which is very important for comparison with experimental data. We first calculate the delay time by which the generation lags the beginning of the pump pulse. Up to the initiation of generation ( $y = 0$ ) we obtain

$$\begin{aligned} x &= A_1 \exp(\lambda_1 t) + A_2 \exp(\lambda_2 t) + x_0, \\ \delta &= B_1 \exp(\lambda_1 t) + B_2 \exp(\lambda_2 t) + \delta_0, \end{aligned} \quad (3)$$

where

$$\begin{aligned} \lambda_{1,2} &= -(W + a_1 + a_2 + a_3) \pm [(W + a_1 + a_2 + a_3)^2 \\ &\quad - 3(a_1 a_2 + a_1 a_3 + a_2 a_3 + W(a_2 + a_3))]^{1/2}, \end{aligned}$$

$$A_1 = x_p - x_0 - A_2,$$

$$A_2 = \frac{1}{\lambda_2 - \lambda_1} [\delta_p W - \lambda_1(x_p - x_0)],$$

$$B_1 = \frac{\lambda_1 + a_2 + 2a_3}{a_1 - a_2 + W} A_1,$$

$$B_2 = \frac{\lambda_2 + a_2 + 2a_3}{a_1 - a_2 + W} A_2,$$

$$x_0 = x_p + \frac{\delta_p [W - (a_1 - a_2)\beta]}{(a_2 + 2a_3)(1 + \beta)},$$

$$\delta_0 = \frac{\delta_p}{1 + \beta}, \quad \beta = W \frac{a_2 + a_3}{a_1 a_2 + a_1 a_3 + a_2 a_3}.$$

The parameter  $\beta$  is the factor of saturation of the auxiliary  $1 \rightarrow 3$  transition by the pump field. Taking the population differences  $x$  and  $\delta$  in (3) as

the different threshold values under steady saturation conditions, we obtain for the delay time the formula

$$B_1 \exp(\lambda_1 t_d) + B_2 \exp(\lambda_2 t_d) = \frac{\delta_p(\beta - \beta_{01})}{(1 + \beta_{01})(1 + \beta)}, \quad (4)$$

where  $\beta_{01}$  is the saturation factor of the  $1 \rightarrow 3$  transition with threshold pump power. If we take the relaxation probabilities between all levels to be the same ( $a_1 = a_2 = a_3 = a$ ), we obtain a simpler formula<sup>1)</sup> for  $t_d$

$$\frac{t_d}{T_1} = \ln \left( \frac{1 + \beta_{01}}{1 - P_0/P} \right) \left/ \left( 1 + \beta_{01} \frac{P}{P_0} \right) \right., \quad (4a)$$

where  $T_1 = 1/3a$  is the spin-lattice relaxation time.

We consider now the transient oscillations in a PM. We linearize Eq. (1). Setting

$$x = x_0 + \Delta x, \quad \delta = \delta_0 + \Delta \delta, \quad y = y_0 + \Delta y,$$

for  $\Delta x/x_0$ ,  $\Delta \delta/\delta_0$ ,  $\Delta y/y_0 \ll 1$  we obtain

$$\begin{aligned} \Delta \dot{x} &= -(a_2 + 2a_3 + 2y_0)\Delta x - 2x_0\Delta y + (W + a_1 - a_2)\Delta \delta, \\ \Delta \dot{\delta} &= (a_3 - a_2 + y_0)\Delta x + x_0\Delta y - (2W + 2a_1 + a_2)\Delta \delta, \\ \Delta \dot{y} &= \alpha y_0 \Delta x. \end{aligned} \quad (5)$$

The steady-state values  $x_0$ ,  $\delta_0$ , and  $y_0$  determined from (1) (for  $\dot{x} = \dot{\delta} = \dot{y} = 0$ ) are

$$\begin{aligned} x_0 &= \frac{1}{\alpha \tau_p}, \quad \delta_0 = \frac{(a_1 + a_2)\delta_p - a_2(x_0 - x_p)}{a_1 + a_2 + W}, \\ y_0 &= a_2 \delta_p \left( \frac{P}{P_0} - 1 \right) \left/ x_0 (1 + \beta_{02}) \left( \frac{P}{P_0} + \frac{a_1 + a_2}{W_{02}} \right) \right. \end{aligned} \quad (6)$$

where  $P/P_0 = W/W_{02}$ ;  $W_{02}$  is the transition probability  $1 \rightarrow 3$  at threshold in the steady-state regime (for  $y_0 = 0$ );  $\beta_{02} = w_{02}(a_2 + a_3)/(a_1 a_2 + a_1 a_3 + a_2 a_3)$  is the saturation factor of the  $1 \rightarrow 3$  transition under threshold pump power. Equations (5) have a solution in the form

$$\begin{aligned} \Delta x &= \sum_{j=1}^3 A_j \exp(\gamma_j t), \\ \Delta \delta &= \sum_{j=1}^3 B_j \exp(\gamma_j t), \\ \Delta y &= \sum_{j=1}^3 C_j \exp(\gamma_j t), \end{aligned} \quad (7)$$

where  $A_j$ ,  $B_j$ ,  $C_j$  are constants determined by the initial conditions, and  $\gamma_j$  are roots of the characteristic equation

<sup>1)</sup>Here we have used the relation  $\beta/\beta_{01} = W/W_{01} = P/P_0$ .

$$\begin{aligned}
 f(\gamma) &= \gamma^3 + 2(W + a_1 + a_2 + a_3 + y_0)\gamma^2 \\
 &+ \{3[W(a_2 + a_3) + a_1a_2 + a_1a_3 + a_2a_3] \\
 &+ 3(W + a_1 + a_2)y_0 + 2\alpha x_0 y_0\}\gamma \\
 &+ 3\alpha x_0 y_0(W + a_1 + a_2) = 0.
 \end{aligned}
 \tag{8}$$

The approximate solution of Eq. (8) gives

$$\gamma_{1,2} = K \pm i\Omega, \quad \gamma_3 = -\frac{3}{2}(W + a_1 + a_2), \tag{9}$$

where

$$\begin{aligned}
 K &= [1/4(W + a_1 + a_2) + y_0 + a_3], \\
 \Omega^2 &= 2\alpha x_0 y_0 + 3(W + a_1)a_2 - 1/16(W + a_1 + a_2)^2 - K^2.
 \end{aligned}$$

Therefore the solutions (7), which describe the transitional process of establishing oscillations in a PM with approach to stationary conditions with constant pumping ( $W = \text{const}$ ), contain a term with decaying oscillations (roots  $\gamma_{1,2}$ ) with rate of decay  $K$  and oscillation frequency  $\Omega$  and a term with exponential damping (root  $\gamma_3$ ). From Eqs. (2), (6), (7), and (9) we obtain for the power radiated by the active paramagnetic crystal,

$$\begin{aligned}
 P_{\text{rad}} &= P_{\text{rad}}^0 \left\{ 1 + \frac{A}{y_0} [1 + (\Omega + K)\tau_p] \exp(Kt) \sin(\Omega t + \varphi) \right. \\
 &\left. + \frac{B}{y_0} \exp(\gamma_3 t) \right\}
 \end{aligned}
 \tag{10}$$

where the constants  $A$ ,  $B$ , and  $\varphi$  are determined by the initial conditions, and the emitted power in steady state is  $P_{\text{rad}}^0 = h\nu_{21}x_0y_0$ .

It is seen from (10) and (6) that an important role is played by the saturation effect in three-level PM's. The power emitted in steady state tends to a constant value as the pump power is increased. The character of the dependence of the frequency of the transitional oscillations on the pump power is likewise essentially determined by the saturation effect. The values of the parameters that characterize the rate of the transient in a PM can be represented in a form convenient for comparison with experiment, if it is assumed that the probabilities for relaxation transitions between all the energy levels are the same:

$$\begin{aligned}
 (a_1 = a_2 = a_3 = a = 1/3T_1): \\
 K &= - \left[ \frac{1}{2T_1} + \frac{\beta_{02}}{8T_1} \frac{P}{P_0} + y_0 \right], \\
 \Omega^2 &= 2\alpha x_0 y_0 - 3 \left( \frac{\beta_{02}}{4T_1} \frac{P}{P_0} \right)^2 - K^2, \\
 \gamma_3 &= - \frac{1}{T_1} \left( \frac{3}{4} \beta_{02} \frac{P}{P_0} + 1 \right),
 \end{aligned}
 \tag{11}$$

where

$$\begin{aligned}
 y_0 &= \delta_p \left( \frac{P}{P_0} - 1 \right) / 3x_0T_1(1 + \beta_{02}) \left( \frac{P}{P_0} + \frac{4}{3\beta_{02}} \right), \\
 \delta_p &= \frac{Nh\nu_{31}}{3kT} \quad \text{for} \quad \frac{h\nu_{31}}{kT} \ll 1,
 \end{aligned}$$

$N$  is the number of  $\text{Cr}^{3+}$  ions in the crystal.

We given also the formula for the output power of the PM in steady state:

$$\begin{aligned}
 P_{\text{out}}^0 &= \epsilon P_{\text{rad}}^0 \\
 &= \epsilon h\nu_{21} \delta_p \left( \frac{P}{P_0} - 1 \right) / 3T_1(1 + \beta_{02}) \left( \frac{P}{P_0} + \frac{4}{3\beta_{02}} \right),
 \end{aligned}
 \tag{12}$$

where  $\epsilon$  is the coupling coefficient of the resonator with the external line. Equations (4a), (11), and (12) were compared with experiment; they described rather well the observed dependence of the quantities

$$t_d, \quad T_{\text{osc}} = 2\pi / \Omega, \quad \tau = 1 / |K|, \quad \tau_e = 1 / |\gamma_3|,$$

which characterize the various stages of the transient and the steady-state oscillation amplitudes of the ruby and rutile masers on the pump power. To illustrate, we show in Fig. 4 the generation delay time and the frequency of the transient oscillations in the ruby maser as a function of pump power. For quantitative comparisons of Eqs. (4a), (11), and (12) with experiment, we used the following values of the quantities appearing in them: For the ruby maser:  $\beta_{01} = 15$ ,  $T_1 = 60$  msec,  $\beta_{02} = 36$ ,  $\alpha = 7.5 \times 10^{-8} \text{ sec}^{-1}$ ,  $\tau_p = 2.2 \times 10^{-7} \text{ sec}$ ,  $N = 8 \times 10^{18}$ ,  $\nu_{21} = 1.4$  Gcs,  $\nu_{31} = 11.3$  Gcs,  $\epsilon \approx 0.5$ . For the rutile maser:  $\beta_{01} \approx \beta_{02} = 5$ ,  $T_1 = 2.5$  msec,  $\alpha = 8 \times 10^{-7} \text{ sec}^{-1}$ ,  $\tau_p = 0.8 \times 10^{-7} \text{ sec}$ ,  $N = 1.5 \times 10^{18}$ ,  $\nu_{21} = 3.8$  Gcs,  $\nu_{31} = 36.4$  Gcs,  $\epsilon \approx 0.5$ . With these values, Eqs. (4a), (11), and (12) give values for  $t_d$ ,  $T_{\text{osc}}$ ,  $\tau$ ,  $\tau_e$ , and  $P_{\text{out}}^0$  that are close to the measured values. It should be mentioned that all constants, with the exception of  $\alpha$ , can be measured directly and independently. The given values of the concentration of  $\text{Cr}^{3+}$  ions in the ruby and rutile crystals and of the frequencies of the signal

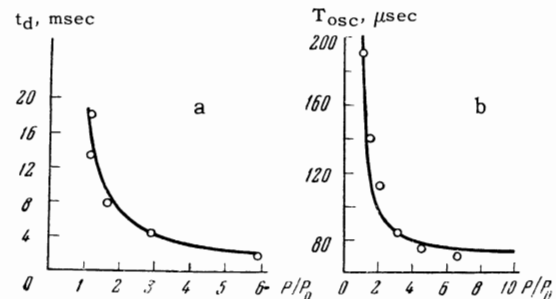


FIG. 4. Dependence on pump power in the ruby maser: a – generation delay time; b – period of the oscillations. Continuous curve, calculated; circles, experimental points.

and pump were measured directly. The saturation factor  $\beta_{01}$  of the  $3 \rightarrow 1$  transition under threshold pump power was not measured directly but was determined by Eq. (4a) from the generation delay time of the PM and the known magnitude of the spin-lattice relaxation time  $T_1$ , measured by the method of pulse saturation of the paramagnetic resonance line. The saturation factor  $\beta_{02}$  was determined from the relation  $\beta_{02} = \beta_{01}P_{02}/P_{01}$ , in which  $P_{01}$  and  $P_{02}$  are the values of the threshold pump power for the non-stationary and stationary generation regimes, i.e., respectively for  $P_{\text{Out}} = 0$  and  $P_{\text{Out}}^0 = 0$ . It is interesting to note that in the ruby maser the threshold pump powers in the stationary and non-stationary regimes are markedly different:  $P_{02}/P_{01} \approx 2.4$ . In the rutile maser  $P_{02}$  and  $P_{01}$  are practically the same. The values of the parameter  $\alpha$ , which characterizes the effectiveness of the interaction of the paramagnetic substance with the radiation field in the resonator, were chosen so as to satisfy the measured values of the oscillation frequency.

Thus, the theory presented here describes rather well the observed transients in PM's. It should be emphasized, however, that the linear approximation is valid only for small deviations from the stationary state and cannot be used to describe exactly the entire process. In particular, in the linear approximation it is impossible to determine the maximum amplitude of the oscillations. As is seen from the experimental data presented (see Fig. 2), one observes in the ruby maser oscillations with large amplitude, comparable or even greater than the stationary generation amplitude. For large deviations of the population differences and generation amplitude from the stationary values, nonlinear effects should become very important. In the ruby maser these nonlinear effects are manifested in the non-sinusoidal form of the oscillations at the start of the transient (see Fig. 2b):

the length of the first peaks is markedly less than the length of the peaks near the stationary level, where the oscillations approach the sinusoidal form.

<sup>1</sup>J. C. Kemp, *J. Appl. Phys.* **30**, 1451 (1959).

<sup>2</sup>A. Yariv, *J. Appl. Phys.* **31**, 740 (1960).

<sup>3</sup>J. R. Singer, *Quantum Electronics*, Columbia University Press, N. Y., 1960.

<sup>4</sup>H. Statz and G. A. de Mars, *Quantum Electronics*, Columbia Univ. Press, New York, 1960, p. 530.

<sup>5</sup>J. R. Singer and S. Wang, *Phys. Rev. Letters* **6**, 351 (1961).

<sup>6</sup>R. W. Hellwarth, *Phys. Rev. Letters* **6**, 9 (1961).

<sup>7</sup>J. C. Kemp, *Phys. Rev. Letters* **7**, 21 (1961).

<sup>8</sup>Kaiser, Garrett, and Wood, *Phys. Rev.* **123**, 766 (1961).

<sup>9</sup>J. I. Kaplan and R. Zier, *J. Appl. Phys.* **33**, 2372 (1962).

<sup>10</sup>H. A. Bostick and J. R. O'Connor, *Proc. IRE* **50**, 219 (1962).

<sup>11</sup>P. Walsh and G. Kemeny, *J. Appl. Phys.* **34**, 956 (1963).

<sup>12</sup>Tang, Statz, and de Mars, *J. Appl. Phys.* **34**, 2289 (1963).

<sup>13</sup>C. L. Tang, *J. Appl. Phys.* **34**, 2935 (1963).

<sup>14</sup>A. Z. Grasyuk and A. N. Oraevskiĭ, *Radio-tekhnik i ėlektronika* **9**, 524 (1964), *Radio Engineering and Electron Physics* **9**, 424 (1964).

<sup>15</sup>R. M. Martirosyan and A. M. Prokhorov, *PTĖ*, No. 1, 106 (1964), *Instr. and Exptl. Tech.*, No. 1, 108 (1964).

<sup>16</sup>Yu. P. Pimenov and A. M. Prokhorov, *Radio-tekhnik i ėlektronika* **8**, 1642 (1963), *Radio Engineering and Electron Physics* **8**, 1566 (1963).